Robust differentiation of human enteroendocrine cells from intestinal stem cells

Daniel Zeve[1,2], Eric Stas[1], Xiaolei Yin[3,4,#], Sarah Dubois[1,5], Manasvi S. Shah[1,2], Erin P. Syverson[2,6], Sophie Hafner[1], Jeffrey M. Karp[4,7,8], Diana L. Carlone[1,2,8], David T. Breault[1,2,8,*]

[1]Division of Endocrinology, Boston Children's Hospital, Boston, MA 02115, USA

[2]Department of Pediatrics, Harvard Medical School, Boston, MA 02115, USA

[3]David H. Koch Institute for Integrative Cancer Research, Massachusetts Institute of Technology, Cambridge, MA 02139, USA

[4]Center for Nanomedicine and Division of Engineering in Medicine, Department of Medicine, Brigham and Women's Hospital, Harvard Medical School, Harvard-MIT Division of Health Sciences and Technology, Boston, MA 02115, USA

[5]School of Arts and Sciences, MCPHS University, Boston, MA 02115, USA

[6]Division of Gastroenterology, Boston Children's Hospital, Boston, MA 02115, USA

[7]Broad Institute of MIT and Harvard, Cambridge, MA 02142, USA

[8]Harvard Stem Cell Institute, 7 Divinity Avenue, Cambridge, MA 02138, USA

[*]Corresponding author

[#]Current address: Institute for Regenerative Medicine, Shanghai East Hospital, Frontier Science Center for Stem Cell Research, School of Life Sciences and Technology, Tongji University, Shanghai, China

ABSTRACT

Enteroendocrine (EE) cells are the most abundant hormone-producing cells in humans and are critical regulators of energy homeostasis and gastrointestinal function. Challenges in converting human intestinal stem cells (ISCs) into functional EE cells, *ex vivo*, have limited progress in elucidating their role in disease pathogenesis and in harnessing their therapeutic potential. To address this, we employed small molecule targeting of key transcriptional regulators, GATA4, JNK and FOXO1, known to mediate endodermal development and hormone production, together with directed differentiation of human ISCs. We observed marked induction of EE cell differentiation and gut-derived expression and secretion of SST, 5HT, and GIP upon treatment with various combinations of three small molecules: rimonabant, SP600125 and AS1842856. Robust differentiation strategies capable of driving human EE cell differentiation is a critical step towards understanding these essential cells and the development of cell-based therapeutics.

INTRODUCTION

Enteroendocrine (EE) cells are found throughout the gastrointestinal (GI) tract and represent the most abundant hormone-producing cell type within mammals. EE cells, as a whole, secrete a large variety of hormones, including glucose-dependent insulinotropic polypeptide (GIP), serotonin (5HT), and somatostatin (SST), among others[1,2]. In response to physiological and nutritional cues, EE cells, through the production of these various hormones, are responsible for regulating multiple aspects of gastrointestinal activity and nutritional homeostasis[1,2]. Because of this, EE cells have been implicated in the pathogenesis of gastrointestinal diseases such as irritable bowel syndrome and inflammatory bowel disease, as well as metabolic diseases such as type 2 diabetes[3-5].

50 Similar to other mature intestinal epithelial cells, EE cells are derived from ISCs, which reside
51 within the crypts of Lieberkuhn[6]. In recent years, much progress has been made understanding
52 the mechanisms underlying ISC self-renewal and differentiation using 3D-enteroid culture[7-10].
53 Using combinations of growth factors and small molecules targeting specific transcriptional
54 regulators and signaling pathways, intestinal enteroids can either be maintained predominantly
55 as ISCs or differentiated into mature intestinal cells of either the absorptive or secretory
56 lineages[11,12]. For example, maintenance of ISC self-renewal requires activation of canonical Wnt
57 signaling using WNT3a and R-spondin, suppression of bone morphogenic protein (BMP)
58 signaling using Noggin, and inhibition of p38 MAPK signaling using the small molecule
59 SB202190[9-11]. By altering these pathways along with transcriptional regulators, strategies have
60 begun to emerge to direct ISC differentiation into mature intestinal epithelial cell types[8,9,13].
61
62 EE cells, as a class, are defined by expression of the neuroendocrine secretory protein
63 Chromogranin A (CHGA), the specific hormone each produces, and location along the GI
64 tract[2,14-16]. Further, multiple transcription factors are critical for EE cell differentiation and
65 function, including neurogenin 3 (NEUROG3), neuronal differentiation 1 (NEUROD1), and
66 pancreatic and duodenal homeobox 1 (PDX1)[1,2,10,17]. The directed differentiation of human EE
67 cells requires the removal of Wnt ligands and inhibition of Notch signaling but, in contrast to
68 mice, human EE cells do not differentiate in the presence of p38 MAPK inhibitors[9,10,16]. While
69 strong mRNA expression of multiple mature EE markers has been observed, limited data exist
70 showing robust protein expression of EE cell markers using small molecule differentiation
71 protocols[8,9,16,18,19].
72
73 Additional factors and signaling pathways have also been implicated in EE cell formation and
74 function. For example, GATA Binding Protein 4 (GATA4) plays a role in small intestine formation
75 and plays an important role in specifying EE cell identity, including GIP-expressing cells[20,21]. c-

76 Jun N-terminal Kinase (JNK) signaling, which has been implicated in regulating ISCs[22], also
77 regulates endocrine cells through its actions on PDX1[23,24]. Inhibition of Forkhead box protein O1
78 (FOXO1), a transcription factor critical for stem cell function and energy homeostasis[25,26], has
79 been associated with upregulation of multiple endocrine-associated transcription factors and
80 hormones, including NEUROG3 and GIP[27-30]. Finally, BMP4 has been shown to induce the
81 expression of various EE hormones in human intestinal enteroids[16]. However, aside from BMP4,
82 how the above factors impact directed differentiation of EE cells has been largely unstudied.
83
84 Here, we establish robust EE cell differentiation protocols for human duodenal enteroids using
85 various combinations of small molecules (rimonabant, SP600125 and AS1842856) designed to
86 alter the activity of GATA4, JNK, and FOXO1, respectively. Treatment with rimonabant and
87 SP600125 leads to marked induction of *CHGA* expression and a corresponding increase in the
88 number of CHGA-positive (CHGA+) cells, as well as in the expression of multiple hormones,
89 including SST, 5HT, and GIP. Separately, treatment with AS1842856 also induced SST, 5HT,
90 and GIP, with an even stronger induction of CHGA+ cells. Comparing levels of hormone
91 secretion, AS1842856 leads to a greater induction of 5HT secretion, but less GIP, whereas
92 rimonabant and SP600125 leads to a greater induction of GIP secretion, but less 5HT. The
93 combination of AS1842856 treatment followed by rimonabant and SP600125 leads to even
94 higher expression of both *SST*, and increased secretion of GIP and 5HT, when compared to
95 rimonabant and SP600125 treatment alone. Together, these robust EE cell differentiation
96 protocols, using small molecules to target GATA4, JNK, and FOXO1, provide important new
97 insights into human EE cell differentiation, with potentially important implications for
98 understanding disease pathogenesis and development of cell-based therapeutics.
99
100 **RESULTS**
101 **Differentiation Media Induces *CHGA* Expression in Human Enteroids**

102 To optimize human EE cell differentiation, we developed a differentiation media (DM,
103 Supplementary Table 1) by combining specific components from published protocols used to
104 induce EE cells[9,12,16,19], including Wnt3a and two additional small molecules associated with
105 endocrine cell differentiation: (1) betacellulin, a ligand of both EGFR and the ErbB4 receptor[31,32]
106 and (2) PF06260933 (PF), a small molecule inhibitor of MAP4K4[33]. Human enteroids were first
107 cultured in growth media (GM, Supplementary Table 1) for two days, allowing for ISC
108 expansion, followed by DM for 12 days (G2D12). Enteroids maintained for 14 days in GM (G14)
109 were used as controls to assess for changes in gene expression. In contrast to previous
110 strategies aimed at generating EE cells over a five day period[9,16], exposure to DM for 12 days
111 was compatible with maintenance of enteroid structural integrity (Fig 1a), possibly due to the
112 continued presence of WNT3a.
113
114 To quantify the effectiveness of DM to induce EE cell differentiation, we profiled the gene
115 expression of *CHGA* and other lineage markers, including mucin 2 (*MUC2*, goblet cells),
116 lysozyme (*LYZ*, Paneth cells), intestinal alkaline phosphatase (*ALPI*, enterocytes) and leucine-
117 rich repeat-containing G-protein coupled receptor 5 (*LGR5*, ISCs). In addition, we assessed the
118 expression of transcription factors required for EE differentiation and function (*PDX1,*
119 *NEUROG3*, and *NEUROD1*), as well as hormones secreted from the duodenum (*SST* and *GIP*).
120 To allow for relative comparison to native tissue expression levels, total RNA from whole
121 mucosal biopsies was included in each qPCR analysis. Exposure of enteroids to G2D12
122 induced consistent expression of *CHGA, SST*, and *GIP*, with significantly higher levels of *ALPI*
123 and significantly lower expression of *LGR5* when compared to G14 (Fig 1b and Supplementary
124 Fig 1a). Despite G2D12's ability to induce EE and enterocyte markers when compared to G14,
125 their overall expression levels remained considerably lower than whole mucosa. Levels of
126 *PDX1*, *NEUROD1*, *NEUROG3*, *GIP*, and *LYZ* were unchanged compared to G14, with *MUC2*
127 showing a trend towards higher expression in G2D12 enteroids (Fig 1b and Supplementary Fig

128 1a). Finally, despite induction in *CHGA* mRNA levels in response to G2D12, analysis of CHGA
129 protein using immunofluorescent staining and flow cytometric analysis revealed fewer than 0.1%
130 of all cells to be CHGA+, showing a trend towards higher expression compared with G14 (Fig
131 1b-1e).
132
133 Removal of WNT3a has been shown to aid EE differentiation[9,10,16]. Analysis of enteroids
134 cultured in DM without WNT3a (G2D12-Wnt) revealed undetectable expression levels of *CHGA*
135 and *SST*, reduced *MUC2* expression, and increased *ALPI* expression when compared with
136 enteroids differentiated with WNT3a (G2D12+Wnt) (Fig 1f). To determine whether *CHGA*
137 expression was increased at an earlier time-point during the 14 day differentiation protocol, we
138 performed time-course studies and found that *CHGA* expression was undetectable in enteroids
139 cultured in G2D12-Wnt, while those exposed to G2D12+Wnt showed expression after six days
140 of starting DM (Supplementary Fig 1b). Furthermore, two of the three enteroid lines exposed to
141 G2D12-Wnt showed low total RNA levels around the eighth day of differentiation, consistent
142 with failure to maintain these lines (Supplementary Fig 1c). Therefore, we concluded that the
143 presence of WNT3a in DM is necessary to sustain enteroids in long-term culture (14 days) and
144 is not detrimental to EE differentiation. We also evaluated the impact of including betacellulin
145 and PF in our DM and found that both factors led to increased expression of EE cell markers
146 compared with GM and DM without betacellulin or PF (Supplementary Fig 1d and 1e). Together,
147 these data indicate that our differentiation protocol markedly induced expression of some EE
148 cell marker genes (e.g., *CHGA*), but is not sufficient to induce a significant increase in the
149 number of CHGA+ EE cells compared to undifferentiated controls.
150
151 **Treatment with Rimonabant and SP600125 Induces EE Lineage Differentiation**
152 To identify additional strategies that might further induce EE cell differentiation, we focused on
153 small molecules shown to target GATA4 and PDX1 activity, key transcriptional regulators

154 involved in gastrointestinal development and hormone regulation. First, we utilized rimonabant
155 (Rim), a highly selective cannabinoid receptor type I antagonist structurally identical to
156 Compound 7, which was previously shown to increase GATA4 activity *in vitro*[34]. In parallel, we
157 used the small molecule SP600125 (SP) to inhibit JNK, which has been shown to suppress
158 PDX1 activity[23,24].
159
160 Separately, both Rim and SP induced expression of multiple EE lineage markers (*CHGA,*
161 *NEUROD1, NEUROG3, SST*, and *GIP*) when added to DM, with Rim having a much larger
162 effect (Supplementary Fig 2a). Together, the combination of Rim and SP (RSP) yielded even
163 further increases in *SST* and *GIP* expression compared to Rim or SP alone. Both PDX1 and
164 GATA4 expression were unchanged under all experimental conditions (Supplementary Fig 2a).
165 Based on these results, Rim and SP were used in combination for all subsequent experiments.
166 The addition of RSP to DM maintained overall enteroid structural integrity during the 14-day
167 differentiation protocol (Fig 2a and Supplementary Fig 2b). Moreover, compared to enteroids
168 grown in G14 and G2D12, treatment with RSP led to the upregulation of multiple EE markers
169 (*CHGA, PDX1, NEUROD1, NEUROG3, SST*, and *GIP*) to levels approximating whole mucosa
170 (Fig 2b). Other lineage markers were also increased with RSP exposure, including *MUC2*, *ALPI*,
171 and *LGR5* when compared to G14 and G2D12 (Supplementary Fig 2c). Immunofluorescent
172 staining for CHGA showed multiple positive cells within individual enteroids (Fig 2c), with a large
173 majority of enteroids (83%) containing CHGA+ cells (Fig 2d). By comparison, only 1% of
174 enteroids grown in G2D12 were CHGA+ (Fig 2D). Quantitative flow cytometric analysis revealed
175 ~1.3% of all cells treated with RSP were CHGA+, almost seven times the number seen with
176 G2D12 alone (Fig 2e).
177
178 **Treatment with AS1842856 Induces EE Lineage Differentiation**

179 Next, we assessed the impact of adding AS1842856 (AS), a well-described FOXO1 inhibitor[35],
180 to our differentiation protocol on the differentiation of EE cells. Addition of AS led to the
181 formation of small, spherical enteroids (Fig 3a and Supplementary Fig 3a). Compared to
182 enteroids grown in G14 and G2D12, AS treatment led to the upregulation of multiple EE
183 markers (*CHGA, PDX1, NEUROD1, NEUROG3, and SST*) to levels approximating whole
184 mucosa (Fig 3b). In addition, AS increased expression of other secretory and ISC markers,
185 including *MUC2*, *LYZ*, and *LGR5*, when compared to G14 and G2D12 (Supplementary Fig 3b).
186 Interestingly, the use of AS reduced expression of the enterocyte marker *ALPI,* when compared
187 to G14 and G2D12, suggesting a possible role for FOXO1 inhibition in the induction of the
188 secretory lineage (Supplementary Fig 3b). Immunofluorescent staining revealed CHGA+ cells
189 within a large majority of individual enteroids (85%) (Fig 3c and 3d). By comparison, only 3% of
190 enteroids grown in G2D12 had CHGA+ cells (Fig 3d). Quantitative flow cytometric analysis
191 revealed ~5.6% of all cells exposed to AS to be CHGA+, almost 50 times the number seen with
192 G2D12 alone (Fig 3e).
193
194 **Treatment with AS1842856 Followed by Rimonabant and SP600215 Increases GIP**
195 **Expression**
196 Compared to RSP-treated enteroids, AS treatment led to more robust EE differentiation, based
197 on overall induction of multiple EE cell markers and the larger fraction of CHGA+ cells (Fig 2
198 and 3). Direct comparison of the two protocols revealed that AS exposure led to higher
199 expression of *CHGA, NEUROD1*, *NEUROG3*, and *SST* (Supplementary Fig 4a), consistent with
200 the higher percentage of CHGA+ cells (Fig 2d and 3d). In addition, we noted that RSP induced
201 higher expression of *GIP* compared to AS (Supplementary Fig 4a). Given these results, we next
202 hypothesized that the combination of Rim, AS, and SP (RASP) would further increase
203 expression of both CHGA and GIP. Exposure of enteroids to RASP for the full duration of the

204 differentiation protocol, however, was not compatible with viable enteroids, as evidenced by
205 their irregular structures and extremely low RNA content (Supplementary Fig 4b and 4c).
206
207 We next tested the impact of adding RSP after exposure to AS, reasoning that AS treatment
208 would shunt a larger proportion of cells into the EE lineage, with the later addition of RSP
209 inducing GIP expression in more cells than RSP alone. To identify the appropriate time for the
210 addition of RSP, we performed a time-course analysis of AS-treated enteroids and found that
211 multiple transcription factors required for EE differentiation, including *NEUROD1* and
212 *NEUROG3*, showed increased expression around the fourth day of differentiation. Following
213 this, both *CHGA* and *SST* had detectable transcript levels by the sixth day of differentiation
214 (Supplementary Fig 5a). Given these data, we next hypothesized that AS treatment for six days
215 followed by subsequent exposure to RSP would lead to increased *GIP* expression compared to
216 RSP alone. To test this, we utilized two differentiation strategies: (1) switching from AS to RSP
217 at day six of differentiation (AS→RSP) or (2) adding RSP to AS at day six of differentiation
218 (AS→RASP). Morphologically, AS→RASP produced smaller enteroids compared to other
219 conditions (Supplementary Fig 5b); however, RNA concentrations were consistently above the
220 minimum threshold of 10ng/μL, suggesting improved viability over exposure to RASP for the full
221 duration of the differentiation protocol (Supplementary Fig 5c). Enteroids treated with
222 AS→RASP showed 2-3-fold higher gene expression levels of most EE cell markers when
223 compared to AS (Fig 4a). In contrast, enteroids treated with AS→RSP showed gene expression
224 changes that were either similar or higher than RSP alone but were significantly lower when
225 compared to AS alone, aside from *PDX1* (Fig 4a). Interestingly, although AS→RSP induced
226 expression of *GIP* similar to RSP alone, AS→RASP induced expression levels significantly less
227 than RSP alone (Fig 4a). Furthermore, exposure to AS for the entire differentiation protocol, i.e.,
228 AS and AS→RASP, decreased expression of *MUC2* and *ALPI* and increased expression of

229 *LGR5* compared to those that received RSP alone, for any amount of time (Supplementary Fig
230 5d).
231
232 All four differentiation strategies induced a high fraction of CHGA+ enteroids, ranging from 79 to
233 88% (RSP, 79%; AS, 82%; AS→RSP, 81%; AS→RASP, 88%), as assessed by immunostaining
234 (Fig 4b and 4c). Quantitative flow cytometric analysis revealed ~3.6% of all cells exposed to
235 AS→RSP to be CHGA+, which is between the 1.0% seen in RSP alone and the 6.0% seen in
236 AS alone. AS→RASP had the highest percentage of CHGA+ cells at 7.0%, more than 100 times
237 the number seen with G2D12 alone (Fig 4d). These data reveal that exposure of human
238 enteroids to AS→RASP is the most effective way to induce EE cell differentiation, in terms of
239 mRNA expression of *CHGA*, *NEUROD1*, and *NEUROG3* as well as overall number of CHGA+
240 cells.
241
242 **Hormone Production and Secretion Mirror Gene Expression Changes**
243 To assess hormone production and secretion during EE cell differentiation, we next assayed for
244 duodenal-associated hormones in response to the various differentiation conditions.
245 Immunofluorescent staining showed that SST was expressed similarly in all differentiation
246 conditions, aside from G2D12, with 42 to 53% of enteroids containing SST-positive cells (RSP,
247 45%; AS, 42%; AS→RSP, 53%; AS→RASP, 51%) (Fig 5a and 5b). 5HT was expressed in a
248 higher percentage of enteroids treated with AS throughout the entire differentiation period than
249 those that only received RSP (RSP, 44%; AS, 75%; AS→RSP, 59%; AS→RASP, 76%) (Fig 5c
250 and 5d). Further, an induction in GIP-positive enteroids was detected in response to all
251 differentiation conditions, with the exceptions of G2D12 and AS→RASP (RSP, 66%; AS, 53%;
252 AS→RSP, 56%; AS→RASP, 10%) (Fig 5e and 5f).
253

254 Finally, to assess hormone secretion, we assayed conditioned media from each differentiation
255 condition. Exposure to AS alone induced higher levels of 5HT secretion than all other
256 conditions, with AS→RSP conditioned media showing higher levels of 5HT when compared to
257 RSP and AS→RASP (Fig 6a). These patterns persisted when corrected for total DNA content,
258 except that there was only a modest difference between AS→RSP and AS→RASP
259 (Supplementary Fig 6a). Secretion of GIP was highest following exposure to AS→RSP,
260 compared to RSP alone, while AS and AS→RASP treated enteroids revealed no secretion of
261 GIP (Fig 6b and Supplementary Fig 6b). Overall, these data show that RSP and AS, either
262 alone or in combination, can induce protein expression and secretion of multiple duodenal
263 hormones in human enteroids, with specific differences seen between 5HT and GIP depending
264 on RSP and AS exposure.
265
266 **DISCUSSION**
267 Here, we establish that the addition of the small molecules rimonabant, SP600125 and
268 AS1842856 leads to robust differentiation of human EE cells from duodenal ISCs without the
269 use of transgenic modification. Prior to this, the differentiation of EE cells using only small
270 molecules had mainly been studied in the context of Wnt, Notch, MAPK and BMP signaling, with
271 inhibition of these pathways driving gastrointestinal stem cells into the secretory lineage, and
272 subsequent removal of p38 MAPK inhibition leading to EE cell differentiation[9,16]. Despite these
273 important advances, the overall efficiency of EE differentiation in the majority of these studies is
274 hard to estimate due to their strong reliance on gene expression analysis with little data at the
275 protein level. In this study, we show robust induction of EE differentiation, assessed using gene
276 and protein expression as well as hormone secretion, at levels that approach the native
277 duodenal mucosa.
278

279 Many of the studies establishing a role for Wnt, Notch, MAPK, and BMP signaling in EE lineage
280 differentiation have been performed using the enteroid culturing system, which approximates *in*
281 *vivo* growth and development due to its 3D nature. However, there are significant shortcomings
282 to the analyses of intestinal enteroid differentiation that our study has begun to address. First,
283 RNA expression does not always mirror protein expression, as evidenced by the presence of
284 *GIP* mRNA in AS→RASP enteroids (Fig 4a) with little protein expression noted on
285 immunofluorescence (Fig 5e and 5f) and no secreted protein seen on ELISA (Fig 6b). Further,
286 our study suggests that enteroids grown in G14 are not appropriate as the sole reference in
287 differentiation experiments. For example, G2D12, but not G14, treatment induced expression of
288 *CHGA* mRNA (Fig 1b), but the comparison of enteroid mRNA expression levels to whole
289 duodenal mucosa revealed that G2D12 alone induces only a very low level of *CHGA* compared
290 to native tissue. Moreover, immunodetection of CHGA expression revealed significant
291 heterogeneity between individual enteroids, even when cultured under the same experimental
292 conditions, as evidenced by only a small minority of enteroids and cells staining CHGA+ in
293 G2D12 and the variability in hormone expression using immunofluorescence. These results
294 highlight the limitations of current human EE differentiation protocols.
295
296 Multiple EE differentiation protocols using only small molecules have suggested that removal of
297 WNT3a from the base growth medium is critical for secretory lineage differentiation[9,16]. Our
298 results, in contrast, reveal that removal of WNT3a is detrimental to both EE differentiation and
299 long-term viability, as noted by a lack of *CHGA* expression at any time during the differentiation
300 protocol and a marked decrease in total RNA levels with time. This is consistent with a previous
301 study suggesting that maintaining high WNT3a concentrations during differentiation was similar,
302 if not better, at inducing *CHGA* expression than a reduction of WNT3a[19]; however, that study
303 only examined differentiation markers after two days of differentiation. The currently described
304 protocol allows for differentiation over 12 days, much longer than previously published methods

305 utilizing only small molecules[16,19]. Even though our length of culture and the use of different
306 reagents and source materials could be possible explanations, our data indicate that removal of
307 WNT3a is not necessary for human EE cell differentiation.
308
309 We also show that treatment of human enteroids with rimonabant, potentially through activation
310 of GATA4, and in conjunction with a known JNK inhibitor, led to an increase in EE marker
311 expression and EE cell number, compared with G2D12 alone, indicating that GATA4 may play a
312 direct role in human EE differentiation during ongoing epithelial maintenance in the adult
313 intestine. We had similar findings when using a well-described inhibitor of FOXO1, which has
314 been previously implicated in beta cell differentiation[29], but whose role in EE cell differentiation
315 has not been closely examined. It is notable that two recent single cell RNA sequencing studies
316 analyzing human and murine EE lineage differentiation using inducible expression of
317 neurogenin 3 did not identify GATA4, JNK, or FOXO1[15,36], suggesting that they may work
318 upstream of neurogenin 3 or that Rim, SP, and AS are all having off target effects in our
319 enteroid model. For example, while Rim is structurally identical to a described GATA4
320 activator[34] and induces increased expression of *GIP*, a known target of GATA4[20], it also
321 functions as a dual inhibitor of sterol O-acyltransferase 1 (SOAT1 or ACAT1) and SOAT2
322 (ACAT2)[37], though these play more of a role in the production of steroid, not peptide,
323 hormones[38].
324
325 Our protocol using the small molecules Rim, SP, and AS showed high levels of human EE cell
326 differentiation compared with prior reports[9,16,19]. While transgenic over-expression of *NEUROG3*
327 generated elevated levels of human EE cells[14,36,39], our method avoids the use of genetic
328 techniques while maintaining EE marker expression at levels at or above endogenous levels
329 within the human duodenal mucosa.
330

331 Interestingly, exposure of enteroids to combinations of Rim, SP, and AS led to the expression of
332 specific hormones, with Rim and SP inducing GIP expression and AS inducing higher levels of
333 5HT expression. Exposure to AS→RSP yielded similar levels of GIP mRNA and total GIP+
334 enteroids, but increased levels of GIP secretion, when compared to RSP alone; however,
335 AS→RASP seemingly inhibited GIP protein production and secretion. AS alone appears to be
336 the most potent inducer of 5HT secretion. Exposure to RSP, with or without AS, induced less
337 5HT secretion when compared to AS alone. Taken together, these combinatorial data suggest
338 that AS exposure is a potent inducer of 5HT secretion while inhibiting GIP secretion, and
339 exposure to Rim and SP is a potent inducer of GIP secretion while leading to reduced 5HT
340 secretion, when compared to AS-treated enteroids. These data suggest that modulation of
341 GATA4, JNK, and FOXO1, as well as other possible targets, could have multiple effects on EE
342 function, controlling mRNA and protein production, as well as secretion, of multiple hormones.
343
344 In summary, addition of Rimonabant, SP600125 and AS1842856 leads to robust differentiation
345 of human EE cells from duodenal ISCs, improving on current methods of differentiation without
346 the use of direct genetic alteration. These studies provide a platform for future studies designed
347 to identify endogenous factors regulating EE differentiation, identifying the role/response of EE
348 cells in human GI disease, and further increasing EE cell numbers to potentially be used as
349 personalized cell therapy.
350
351

352 **METHODS**

353 **Isolation of human intestinal crypts**

354 Tissues were procured as previously described [40]. In short, de-identified endoscopic biopsies
355 were collected from grossly unaffected tissues in pediatric patients undergoing
356 esophagogastroduodenoscopy at Boston Children's Hospital for gastrointestinal complaints and
357 used for duodenal enteroid derivation. Further, de-identified duodenal resections were collected
358 from adult patients undergoing pancreaticoduodenectomy at Massachusetts General Hospital
359 prior to chemotherapy or radiation therapy for pancreatic carcinoma. Whole mucosal biopsies
360 were generated from the duodenal resections using endoscopic biopsy forceps and used for
361 total RNA isolation. Age and sex of donors can be found in Supplementary Table 2 but were
362 unknown to researchers when experiments were being performed. Only macroscopically
363 normal-appearing tissue was used from patients without a known gastrointestinal diagnosis.
364 Each experiment was performed on at least three independent enteroid lines derived from
365 pediatric biopsy samples. Informed consent and developmentally appropriate assent were
366 obtained at Boston Children's Hospital from the donors' guardian and the donor, respectively.
367 Informed consent was obtained at Massachusetts General Hospital from the donors. All
368 methods were approved and carried out in accordance with the Institutional Review Boards of
369 Boston Children's Hospital (Protocol number IRB-P00000529) and Massachusetts General
370 Hospital (Protocol number IRB-2003P001289).

371

372 Resections were briefly washed with pre-warmed DMEM/F12, after which the epithelial layer
373 was separated from the rest of the duodenum manually with sterilized surgical tools then taken
374 for RNA isolation. To isolate crypts, pediatric biopsies were digested in 2mg/mL of Collagenase
375 Type I (Life Technologies, 17018029) reconstituted in Hank's Balanced Salt Solution for 40
376 minutes at 37°C. Samples were then agitated by pipetting followed by centrifugation at 500 x g
377 for 5 minutes at 4°C. The supernatant was then removed, and crypts resuspended in 200-300μL

378 of Matrigel (Corning, 356231), with 50µL being plated onto 4-6 wells of a 24-well plate and
379 polymerized at 37°C.
380
381 **Culturing of human duodenal enteroids *in vitro***
382 Isolated crypts in Matrigel were grown in growth media (GM) (Supplementary Table 1) and the
383 resulting enteroids were passaged every 6-8 days as needed, with media changes occurring
384 every two days. To passage, Matrigel was mechanically dissociated from the well and
385 resuspended in 500µL of Cell Recovery solution (Corning, 354253) for 40-60 minutes at 4°C. To
386 aid in separating the Matrigel and enteroids, the tubes are gently inverted and then centrifuged
387 at 500 x g for 5 minutes at 4°C. The supernatant was then removed, and enteroids resuspended
388 in Matrigel, followed by mechanical disruption via a bent-tipped pipette. Enteroids were
389 passaged at a 1:2 dilution, with 50µL per well of a 24-well plate. After plating, the enteroids were
390 incubated at 37°C for 10 minutes to allow the Matrigel to set. Once complete, 500µL of GM was
391 added to each well.
392
393 For differentiation, enteroids were passaged and grown in GM for two days, to allow for ISC
394 expansion, after which the enteroids were transitioned to differentiation media (DM) with
395 additional small molecules added as described (Supplementary Table 1). Media was changed
396 every two days, with Tubastatin A being removed after the second day of differentiation.
397 Enteroids were taken for analysis after 14 days.
398
399 **Gene expression analysis**
400 Total RNA was purified from individual wells using TRI®Reagent (Sigma) and the Direct-zol™
401 RNA kit (Zymo Research), following the manufacturer's protocol. RNA concentration was
402 determined using a NanoDrop™ 1000 spectrophotometer (Life Technologies). RNA was treated

403 with DNAse (Promega) and reverse transcribed using the High-Capacity cDNA Reverse
404 Transcription Kit (Life Technologies). Gene expression analysis was then performed by Real
405 Time quantitative PCR (qPCR) using a QuantStudio 6 Flex thermocycler (Life Technologies).
406 We used the following Taqman primers from Life Technologies (Supplementary Table 3). *18S*
407 transcripts were used as the internal control and data were expressed using the 2^{-ddCt} method
408 with Ct limit of 40. Fold change, unless otherwise stated, was compared to total RNA derived
409 from adult whole mucosal tissue biopsies.
410
411 **DNA isolation**
412 To isolate enteroid genomic DNA, 200μL of 50mM NaOH was added to a single well of a 24-
413 well plate and the Matrigel was mechanically dissociated. The samples were then transferred to
414 1.5mL microcentrifuge tubes and placed in a 95°C heat block for 20 minutes. The tubes were
415 then vortexed, after which 25 μL of 1M Tris-HCl was added. The samples were then centrifuged
416 at 14,000 rpm for 10 minutes. The DNA content of the supernatant was then assayed using a
417 NanoDrop™ 1000 spectrophotometer (Life Technologies).
418
419 **Immunofluorescence**
420 Immunofluorescence staining was performed as previously described with minor
421 modifications[41]. Enteroids were grown in and isolated from Matrigel as noted above. 1-2 wells
422 from a 24-well plate were washed in 200μL of 1X phosphate-buffered saline (PBS) and moved
423 in suspension to a 1.5mL microcentrifuge tube. Each tube was centrifuged at 800 x g for 5
424 minutes at 4°C to pellet enteroids. PBS was aspirated, and enteroids were fixed in 200μL of 4%
425 paraformaldehyde (PFA) for 20 minutes on ice, shaking. Each tube was centrifuged again as
426 above, and PFA was aspirated. The enteroids were then resuspended in 500μL of 0.3% Triton-
427 X in PBS and moved to a 48-well plate for the remaining steps. The enteroids were

428 permeabilized for 30 minutes at room temperature, shaking. Between each step, enteroids were
429 allowed to settle to the bottom of each well, the plate was angled, and the solution aspirated by
430 careful pipetting. Enteroids were then blocked with 5% bovine serum albumin in PBS for 1.5
431 hours at room temperature, shaking. This was followed by three five-minute washes in 500μL of
432 PBS at room temperature, shaking.
433
434 Each well was then incubated in 200μL of primary antibodies diluted in 5% BSA/0.1% Trition-X
435 in PBS at 4°C overnight. Primary antibodies include Chromogranin A (CHGA) (Agilent/Dako,
436 M086901-2, 1:100; Millipore Sigma, HPA017369, 1:100), Serotonin (Abcam, ab66047, 1:100),
437 GIP (Invitrogen, PA5-76867, 1:100) and Somatostatin (R&D Systems, mab2358, 1:100). This
438 was followed by five washes in 500μL of 0.1% Triton-X in PBS for 15 minutes each at room
439 temperature, shaking. 200μL of secondary antibodies, including Alexa Fluor 488- or 647-
440 conjugated anti-mouse (Invitrogen, A-21202, or A-31571, 1:400), Alexa Fluor 488-conjugated
441 anti-rat (Invitrogen, A-21208, 1:400), Alexa Fluor 488-conjugated anti-goat (Invitrogen, A-11055,
442 1:400) or Alexa Fluor 647-conjugated anti-rabbit (Invitrogen, A-31573, 1:400) diluted in 0.1%
443 Triton-X in PBS were then added to each well and incubated for two hours at room temperature,
444 shaking. Enteroids were then washed as above, then moved to new 1.5mL centrifuge tubes.
445 During the last wash, 4′,6-diamidino-2-phenylindole (DAPI, Life Technologies, D1306) was
446 added at a concentration of 1:1000 for nuclear staining. Enteroids were then centrifuged at 1000
447 x g for 5 minutes at 4°C to help remove as much PBS as possible. Slides were prepared by
448 drawing three circles with a hydrophobic pen (Vector Laboratories, H-4000). Enteroids were
449 then resuspended in 20μL of Prolong Gold Antifade mountant (Life Technologies, P36930), and
450 droplets placed within hydrophobic circles. The enteroids were spread out to reduce clumping,
451 sealed with a coverslip, and allowed to dry overnight at room temperature. Slides were stored at

452 4°C for future imaging. Images were acquired using a Nikon upright Eclipse 90i microscope with
453 a 20×/0.75 Plan-Apochromat objective and adjusted for brightness and contrast in Fiji[42].
454
455 **Quantification of immunofluorescent enteroids**
456 This technique was adapted from a previously described method[43]. Immunofluorescent images
457 were acquired using an Invitrogen EVOS FL 2 Auto microscope (Life Technologies).
458 Representative images of stained enteroids were taken at 2X magnification. The stitched
459 images were then processed in Fiji[42]. The color of the DAPI images was converted to 8-bit
460 grayscale and then the image was smoothed by applying a Gaussian Blur filter (radius = 4,
461 scaled units). Thresholding of the smoothed images was performed using manual adjustment to
462 achieve optimal separation of individual enteroids. Watershed and Find Edges filters were then
463 applied to segment any clumped enteroids. Post-segmentation analysis was performed to
464 outline and count individual enteroids using Analyze Particles (size=4,000-100,000,
465 circularity=0.30-1.00, exclude on edges). Each image was then manually curated to exclude
466 debris and enteroids exhibiting background fluorescence. Any remaining clumped enteroids
467 were manually separated prior to quantification. The outlines generated from the DAPI images
468 were then applied to the corresponding images from the other fluorescent channels. Each color
469 image was converted to 8-bit grayscale and then the HiLo Lookup Table was applied. The
470 threshold gate for stained cells was found by manual adjustment of positively stained enteroids
471 to achieve optimal representation. The threshold gate for each channel was then applied to
472 each experimental condition. The Mean metric was extracted with ROI manager (measure) and
473 compiled for analysis. Enteroids with a Mean value of more than zero were considered positive.
474
475 **Flow cytometry**

476 Enteroids were incubated in Cell Recovery solution for 40-60 minutes at 4°C to remove the
477 Matrigel and then centrifuged at 500 x g for 5 minutes at 4°C. Enteroids were then incubated in
478 500µL of TrypLE Express (Life Technologies) at 37°C for 30 minutes and broken up by
479 repeated pipetting using a bent P1000 pipette tip. Each sample was then diluted in 800µL of
480 20% FBS in Advanced DMEM/F12 and then centrifuged at 500 x g for 5 minutes at 4°C. To
481 mark dead cells, each sample was then incubated in DAPI (1:1000) diluted in 2% FBS/2mM
482 EDTA/calcium-free DMEM for 20 minutes at room temperature, then centrifuged at 500 x g for 5
483 minutes at 4°C and washed in 2% FBS/2mM EDTA/DMEM. Cells were then incubated in 1%
484 PFA for 15 minutes at room temperature, washed with 2% FBS/PBS and then permeabilized in
485 0.2% Tween 20 in 2% FBS/PBS for 15 minutes at 37°C. Following centrifugation, cells were
486 resuspended in 0.1% Tween 20/2% FBS/2mM EDTA in PBS with PE-conjugated CHGA (BD
487 Biosciences, 564563, 1:100) or PE-conjugated mouse IgG1, K isotype, (BD Biosciences,
488 554680, 1:200) or with no antibody (the latter two acting as controls) for 30 minutes on ice.
489 Cells were then washed in 0.1% Tween 20/2% FBS/2mM EDTA in PBS, filtered through a 37-
490 micron mesh, and then analyzed on a BD FACSAria II SORP flow cytometer. For gating
491 strategy, please see Supplementary Figure 7.
492
493 **ELISA**
494 Hormone quantification for serotonin (Eagle Biosciences/DLD Diagnostika GmbH, SER39-K01)
495 and GIP (MilliporeSigma, EZHGIP-54K) were performed following manufacturer's protocols. For
496 these experiments, enteroids were grown in 48-well plates to aid in concentrating the hormone
497 of interest. Conditioned media was taken on day 14 of differentiation. For GIP quantification,
498 Diprotin A (Tocris, 6019, 100µM), a dipeptidyl peptidase 4 inhibitor, was added daily to the
499 media for the last two days of differentiation to prevent GIP degradation. As a control,

500 differentiation media not exposed to cells was also evaluated. This value was then subtracted
501 from each experimental sample.
502
503 **Quantification and statistical analysis**
504 All experiments were repeated using at least three different human enteroid lines and
505 representative data from a single line is shown. For qPCR and flow cytometry studies, each
506 condition was performed using pooled enteroids from 3-5 wells, unless otherwise noted, with
507 each well acting as a single sample. Whole mucosal biopsies from duodenal resections were
508 combined from three different individuals to generate a single reference sample for all
509 experiments.
510
511 Prior to statistical analysis, all qPCR data were transformed using $\log_{10}$. When analyzing only
512 two conditions, statistical significance was determined by unpaired, two-tailed Student's t-test,
513 combined with the Holm-Sidak method to control for multiple comparisons. When analyzing
514 more than two conditions, statistical significance was determined by either one-way or two-way
515 ANOVA, followed by Tukey post hoc analysis. Specific conditions were excluded from statistical
516 analysis if the data from 1 or more samples was labeled as not detectable. Statistical details for
517 each experiment can be found within each figure legend.
518
519 **ACKNOWLEDGEMENTS**
520 We thank members of the Breault laboratory, J. Majzoub, S. Bonner-Weir and J. Turner for
521 helpful discussions. This research was supported by National Institute of Health (NIH) awards
522 T32DK769937, K12DK09472109 and Pediatric Endocrine Society Research Fellowship and
523 Clinical Scholar Awards (to D.Z.), NIH awards HL095722 and UC4DK104165 (to J.M.K.), and
524 support from the Adolph Coors Foundation Award (to D.T.B.).
525

AUTHOR CONTRIBUTIONS

D.Z. designed and performed experiments, analyzed data, prepared figures and co-wrote the manuscript; E.S. performed experiments, analyzed data and edited the manuscript; X.Y. and E.P.S. performed cell culture experiments; M.S.S. performed flow cytometry experiments; S.D. and S.H. assisted in qPCR and immunofluorescence experiments; J.M.K. provided conceptual advice and reagents; D.L.C. provided conceptual advice and edited the manuscript, and D.T.B. directed the project and co-wrote the manuscript.

COMPETING INTERESTS

The author J.M.K. holds equity in Frequency Therapeutics, a company that has an option to license IP generated by J.M.K and that may benefit financially if the IP is licensed and further validated. The interests of J.M.K. was reviewed and are subject to a management plan overseen by their institutions in accordance with their conflict of interest policies.

Data Availability

This study did not generate any datasets.

Code Availability

This study did not generate or use any previously unreported custom code.

547 **REFERENCES**

548

549 1 Posovszky, C. Development and Anatomy of the Enteroendocrine System in Humans.
550 *Endocr Dev* **32**, 20-37, doi:10.1159/000475729 (2017).

551 2 Furness, J. B., Rivera, L. R., Cho, H. J., Bravo, D. M. & Callaghan, B. The gut as a sensory
552 organ. *Nat Rev Gastroenterol Hepatol* **10**, 729-740, doi:10.1038/nrgastro.2013.180
553 (2013).

554 3 El-Salhy, M., Hausken, T., Gilja, O. H. & Hatlebakk, J. G. The possible role of
555 gastrointestinal endocrine cells in the pathophysiology of irritable bowel syndrome. *Expert*
556 *Rev Gastroenterol Hepatol* **11**, 139-148, doi:10.1080/17474124.2017.1269601 (2017).

557 4 Worthington, J. J., Reimann, F. & Gribble, F. M. Enteroendocrine cells-sensory sentinels
558 of the intestinal environment and orchestrators of mucosal immunity. *Mucosal Immunol*
559 **11**, 3-20, doi:10.1038/mi.2017.73 (2018).

560 5 Holst, J. J., Vilsboll, T. & Deacon, C. F. The incretin system and its role in type 2 diabetes
561 mellitus. *Mol Cell Endocrinol* **297**, 127-136, doi:10.1016/j.mce.2008.08.012 (2009).

562 6 Yousefi, M., Li, L. & Lengner, C. J. Hierarchy and Plasticity in the Intestinal Stem Cell
563 Compartment. *Trends Cell Biol* **27**, 753-764, doi:10.1016/j.tcb.2017.06.006 (2017).

564 7 Yu, H. *et al.* The Contributions of Human Mini-Intestines to the Study of Intestinal
565 Physiology and Pathophysiology. *Annu Rev Physiol* **79**, 291-312, doi:10.1146/annurev-
566 physiol-021115-105211 (2017).

567 8 Fujii, M. *et al.* Human Intestinal Organoids Maintain Self-Renewal Capacity and Cellular
568 Diversity in Niche-Inspired Culture Condition. *Cell Stem Cell* **23**, 787-793 e786,
569 doi:10.1016/j.stem.2018.11.016 (2018).

570 9 Sato, T. *et al.* Long-term expansion of epithelial organoids from human colon, adenoma,
571 adenocarcinoma, and Barrett's epithelium. *Gastroenterology* **141**, 1762-1772,
572 doi:10.1053/j.gastro.2011.07.050 (2011).

573 10 Basak, O. *et al.* Induced Quiescence of Lgr5+ Stem Cells in Intestinal Organoids Enables
574 Differentiation of Hormone-Producing Enteroendocrine Cells. *Cell Stem Cell* **20**, 177-190
575 e174, doi:10.1016/j.stem.2016.11.001 (2017).

576 11 Sato, T. & Clevers, H. SnapShot: Growing Organoids from Stem Cells. *Cell* **161**, 1700-
577 1700 e1701, doi:10.1016/j.cell.2015.06.028 (2015).

578 12 Yin, X. *et al.* Niche-independent high-purity cultures of Lgr5+ intestinal stem cells and their
579 progeny. *Nat Methods* **11**, 106-112, doi:10.1038/nmeth.2737 (2014).

580 13 Almeqdadi, M., Mana, M. D., Roper, J. & Yilmaz, O. H. Gut organoids: mini-tissues in
581 culture to study intestinal physiology and disease. *Am J Physiol Cell Physiol* **317**, C405-
582 C419, doi:10.1152/ajpcell.00300.2017 (2019).

583 14 Sinagoga, K. L. *et al.* Deriving functional human enteroendocrine cells from pluripotent
584 stem cells. *Development* **145**, doi:10.1242/dev.165795 (2018).

585 15 Gehart, H. *et al.* Identification of Enteroendocrine Regulators by Real-Time Single-Cell
586 Differentiation Mapping. *Cell* **176**, 1158-1173 e1116, doi:10.1016/j.cell.2018.12.029
587 (2019).

588 16 Beumer, J. *et al.* Enteroendocrine cells switch hormone expression along the crypt-to-
589 villus BMP signalling gradient. *Nat Cell Biol* **20**, 909-916, doi:10.1038/s41556-018-0143-y
590 (2018).

591 17 Chen, C., Fang, R., Davis, C., Maravelias, C. & Sibley, E. Pdx1 inactivation restricted to
592 the intestinal epithelium in mice alters duodenal gene expression in enterocytes and
593 enteroendocrine cells. *Am J Physiol Gastrointest Liver Physiol* **297**, G1126-1137,
594 doi:10.1152/ajpgi.90586.2008 (2009).

595 18 Petersen, N. *et al.* Generation of L cells in mouse and human small intestine organoids.
596 *Diabetes* **63**, 410-420, doi:10.2337/db13-0991 (2014).

597 19 VanDussen, K. L. *et al.* Development of an enhanced human gastrointestinal epithelial
598 culture system to facilitate patient-based assays. *Gut* **64**, 911-920, doi:10.1136/gutjnl-
599 2013-306651 (2015).

600 20 Jepeal, L. I., Boylan, M. O. & Michael Wolfe, M. GATA-4 upregulates glucose-dependent
601 insulinotropic polypeptide expression in cells of pancreatic and intestinal lineage. *Mol Cell*
602 *Endocrinol* **287**, 20-29, doi:10.1016/j.mce.2008.01.024 (2008).

603 21 Walker, E. M., Thompson, C. A. & Battle, M. A. GATA4 and GATA6 regulate intestinal
604 epithelial cytodifferentiation during development. *Dev Biol* **392**, 283-294,
605 doi:10.1016/j.ydbio.2014.05.017 (2014).

606 22 Biteau, B., Hochmuth, C. E. & Jasper, H. JNK activity in somatic stem cells causes loss of
607 tissue homeostasis in the aging Drosophila gut. *Cell Stem Cell* **3**, 442-455,
608 doi:10.1016/j.stem.2008.07.024 (2008).

609 23 Kaneto, H. *et al.* Oxidative stress and the JNK pathway in diabetes. *Curr Diabetes Rev* **1**,
610 65-72 (2005).

611 24 Tang, C. *et al.* Glucose-Induced beta-Cell Dysfunction In Vivo: Evidence for a Causal Role
612 of C-jun N-terminal Kinase Pathway. *Endocrinology* **159**, 3643-3654,
613 doi:10.1210/en.2018-00566 (2018).

614 25 Kousteni, S. FoxO1, the transcriptional chief of staff of energy metabolism. *Bone* **50**, 437-
615 443, doi:10.1016/j.bone.2011.06.034 (2012).

616 26 Tothova, Z. & Gilliland, D. G. FoxO transcription factors and stem cell homeostasis:
617 insights from the hematopoietic system. *Cell Stem Cell* **1**, 140-152,
618 doi:10.1016/j.stem.2007.07.017 (2007).

619 27 Roy, S. A. *et al.* Dual regulatory role for phosphatase and tensin homolog in specification
620 of intestinal endocrine cell subtypes. *World J Gastroenterol* **18**, 1579-1589,
621 doi:10.3748/wjg.v18.i14.1579 (2012).

622 28 Garcia-Martinez, J. M., Chocarro-Calvo, A., De la Vieja, A. & Garcia-Jimenez, C. Insulin
623 drives glucose-dependent insulinotropic peptide expression via glucose-dependent
624 regulation of FoxO1 and LEF1/beta-catenin. *Biochim Biophys Acta* **1839**, 1141-1150,
625 doi:10.1016/j.bbagrm.2014.07.020 (2014).

626 29 Bouchi, R. *et al.* FOXO1 inhibition yields functional insulin-producing cells in human gut
627 organoid cultures. *Nat Commun* **5**, 4242, doi:10.1038/ncomms5242 (2014).

628 30 Arriola, D. J., Mayo, S. L., Skarra, D. V., Benson, C. A. & Thackray, V. G. FOXO1
629 transcription factor inhibits luteinizing hormone beta gene expression in pituitary
630 gonadotrope cells. *J Biol Chem* **287**, 33424-33435, doi:10.1074/jbc.M112.362103 (2012).

631 31 Pagliuca, F. W. *et al.* Generation of functional human pancreatic beta cells in vitro. *Cell*
632 **159**, 428-439, doi:10.1016/j.cell.2014.09.040 (2014).

633 32 Harskamp, L. R., Gansevoort, R. T., van Goor, H. & Meijer, E. The epidermal growth factor
634 receptor pathway in chronic kidney diseases. *Nat Rev Nephrol* **12**, 496-506,
635 doi:10.1038/nrneph.2016.91 (2016).

636 33 Zhao, X., Mohan, R., Ozcan, S. & Tang, X. MicroRNA-30d induces insulin transcription
637 factor MafA and insulin production by targeting mitogen-activated protein 4 kinase 4
638 (MAP4K4) in pancreatic beta-cells. *J Biol Chem* **287**, 31155-31164,
639 doi:10.1074/jbc.M112.362632 (2012).

640 34 Valimaki, M. J. *et al.* Discovery of Small Molecules Targeting the Synergy of Cardiac
641 Transcription Factors GATA4 and NKX2-5. *J Med Chem* **60**, 7781-7798,
642 doi:10.1021/acs.jmedchem.7b00816 (2017).

643 35 Yu, F. *et al.* FoxO1 inhibition promotes differentiation of human embryonic stem cells into
644 insulin producing cells. *Exp Cell Res* **362**, 227-234, doi:10.1016/j.yexcr.2017.11.022
645 (2018).

646 36 Beumer, J. *et al.* High-Resolution mRNA and Secretome Atlas of Human Enteroendocrine
647 Cells. *Cell*, doi:10.1016/j.cell.2020.04.036 (2020).

648 37 Netherland, C. & Thewke, D. P. Rimonabant is a dual inhibitor of acyl CoA:cholesterol
649 acyltransferases 1 and 2. *Biochem Biophys Res Commun* **398**, 671-676,
650 doi:10.1016/j.bbrc.2010.06.134 (2010).

651 38 Ferraz-de-Souza, B. *et al.* Sterol O-acyltransferase 1 (SOAT1, ACAT) is a novel target of
652 steroidogenic factor-1 (SF-1, NR5A1, Ad4BP) in the human adrenal. *J Clin Endocrinol*
653 *Metab* **96**, E663-668, doi:10.1210/jc.2010-2021 (2011).

654 39 Chang-Graham, A. L. *et al.* Human Intestinal Enteroids With Inducible Neurogenin-3
655 Expression as a Novel Model of Gut Hormone Secretion. *Cell Mol Gastroenterol Hepatol*
656 **8**, 209-229, doi:10.1016/j.jcmgh.2019.04.010 (2019).

657 40 Kasendra, M. *et al.* Development of a primary human Small Intestine-on-a-Chip using
658 biopsy-derived organoids. *Sci Rep* **8**, 2871, doi:10.1038/s41598-018-21201-7 (2018).

659 41 Dekkers, J. F. *et al.* High-resolution 3D imaging of fixed and cleared organoids. *Nat Protoc*
660 **14**, 1756-1771, doi:10.1038/s41596-019-0160-8 (2019).

661 42 Schindelin, J. *et al.* Fiji: an open-source platform for biological-image analysis. *Nat*
662 *Methods* **9**, 676-682, doi:10.1038/nmeth.2019 (2012).

663 43 Borten, M. A., Bajikar, S. S., Sasaki, N., Clevers, H. & Janes, K. A. Automated brightfield
664 morphometry of 3D organoid populations by OrganoSeg. *Sci Rep* **8**, 5319,
665 doi:10.1038/s41598-017-18815-8 (2018).
666

667

Figure 1

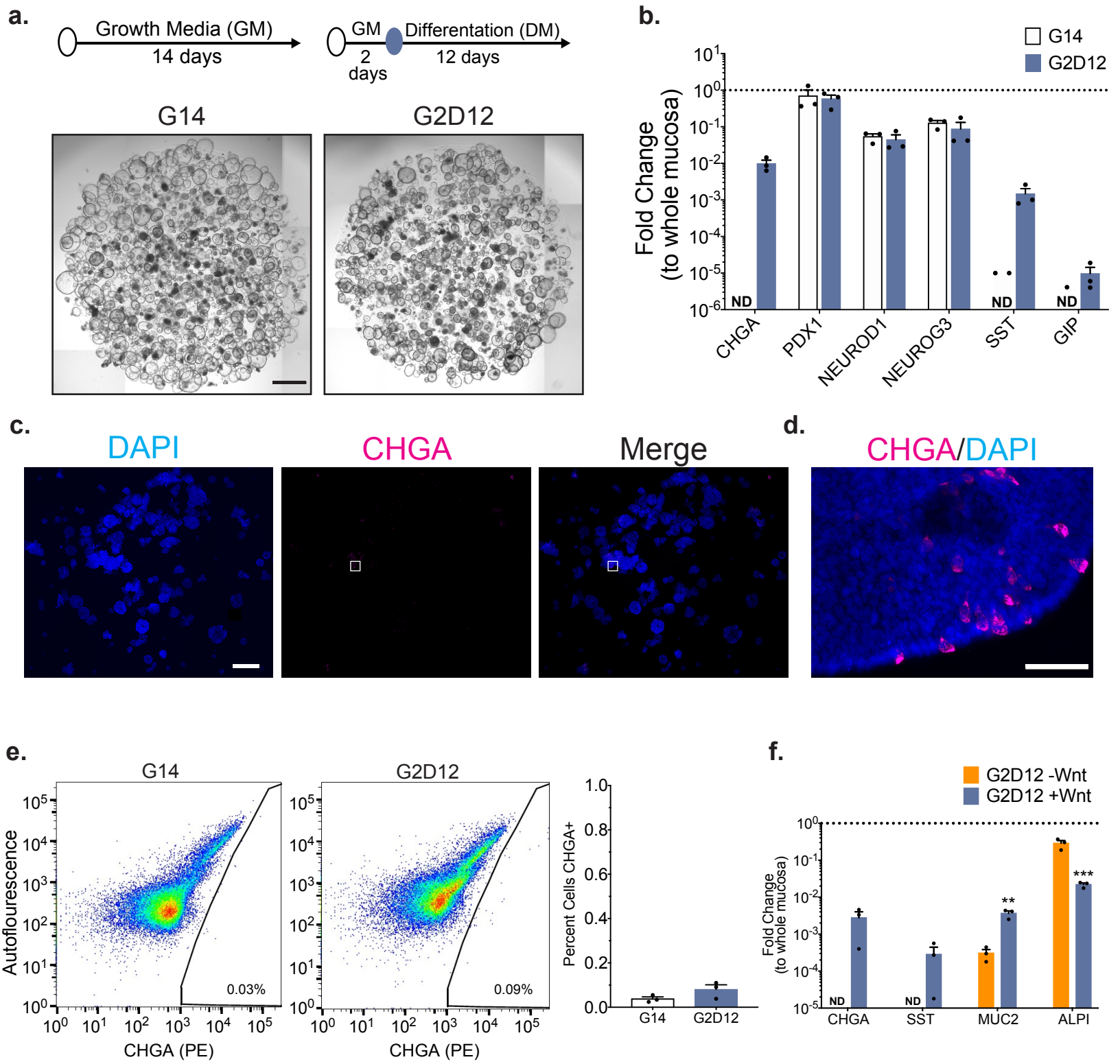
a.
Growth Media (GM)
14 days
GM
2 days
Differentation (DM)
12 days
G14
G2D12
b.
G14
G2D12
Fold Change (to whole mucosa)
ND
CHGA
PDX1
NEUROD1
NEUROG3
SST
GIP
c.
DAPI
CHGA
Merge
d.
CHGA/DAPI
e.
G14
G2D12
Autoflourescence
CHGA (PE)
0.03%
0.09%
Percent Cells CHGA+
f.
G2D12 -Wnt
G2D12 +Wnt
Fold Change (to whole mucosa)
ND
CHGA
SST
MUC2
ALPI
**
***

668 **FIGURE LEGENDS**

669 **Figure 1. Base Differentiation Media Induces CHGA Expression in a Wnt-dependent**
670 **Manner**

671 (a) Representative light microscopy of enteroids (whole well) grown in growth media (GM) for 14
672 days (G14) or two days in GM followed by 12 days in differentiation media (DM, G2D12).
673 Specific culture schematic located above each panel, respectively. Scale bar = 1mm.
674 (b) qPCR analysis of enteroendocrine (EE) markers of enteroids grown in either G14 or G2D12
675 compared to whole mucosa and normalized to *18S*. Dotted line denotes expression level in
676 whole mucosa. Representative experiment showing n = 3 wells for each condition from a single
677 enteroid line. CHGA = chromogranin A, PDX1 = pancreatic and duodenal homeobox 1,
678 NEUROD1 = neuronal differentiation 1, NEUROG3 = neurogenin 3, SST = somatostatin, GIP =
679 glucose-dependent insulinotropic peptide, ND = not detectable in 1 or more samples.
680 (c and d) Representative immunofluorescence staining of CHGA (magenta) in enteroids (whole
681 well) treated with G2D12. Boxed portion in C shown magnified in (D). DNA (4′,6-diamidino-2-
682 phenylindole (DAPI) blue). Scale bars = 1mm (C) and 50μm (D).
683 (e) Left two panels: Representative flow cytometry plots of CHGA-positive (CHGA+) cells from
684 enteroids grown in either G14 or G2D12. Right panel: Percentage of CHGA+ cells per well.
685 Representative experiment showing n = 3 wells from each condition from single enteroid line.
686 (f) qPCR analysis of EE gene markers of enteroids grown in either G2D12 without Wnt (G2D12-
687 Wnt) or with Wnt (G2D12+Wnt) compared to whole mucosa and normalized to *18S*. Dotted line
688 denotes expression level in whole mucosa. MUC2 = Mucin 2, ALPI = Intestinal alkaline
689 phosphatase. Representative experiment showing n = 3 wells from each condition from a single
690 enteroid line.
691 Bars show mean ± SEM, **$p < 0.01$, ***$p < 0.001$. Each experiment repeated with at least three
692 different enteroid lines. Specific conditions were excluded from statistical analysis if the data
693 from 1 or more samples was labeled as not detectable.

Figure 2

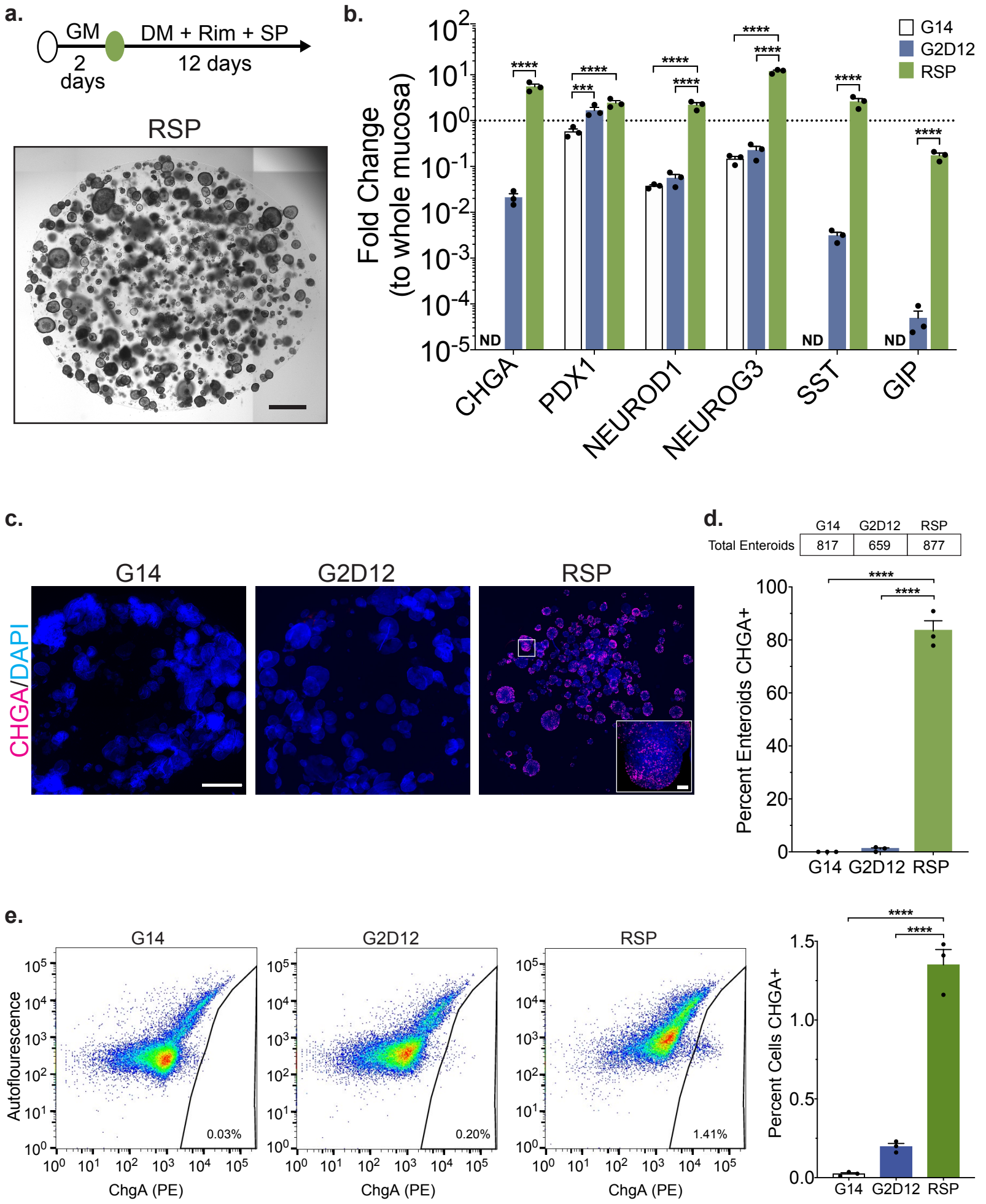
a.
GM
2 days
DM + Rim + SP
12 days
RSP
b.
Fold Change (to whole mucosa)
G14
G2D12
RSP
ND
CHGA
PDX1
NEUROD1
NEUROG3
SST
GIP
c.
G14
G2D12
RSP
CHGA/DAPI
d.
Total Enteroids
G14 817
G2D12 659
RSP 877
Percent Enteroids CHGA+
e.
Autoflourescence
ChgA (PE)
0.03%
0.20%
1.41%
Percent Cells CHGA+

694 **Figure 2. Differentiation with Small Molecules Rimonabant and SP600125 Induces CHGA**
695 **Expression**
696 (a) Representative light microscopy of enteroids (whole well) grown in G2D12 with rimonabant
697 and SP600125 (RSP). Culture schematic located above panel. Scale bar = 1mm.
698 (b) qPCR analysis of enteroendocrine markers of enteroids grown in G14, G2D12 or RSP
699 compared to whole mucosa and normalized to *18S*. Dotted line denotes expression level in
700 whole mucosa. Representative experiment showing n = 3 wells from each condition from a
701 single enteroid line. CHGA = chromogranin A, PDX1 = pancreatic and duodenal homeobox 1,
702 NEUROD1 = neuronal differentiation 1, NEUROG3 = neurogenin 3, SST = somatostatin, GIP =
703 glucose-dependent insulinotropic peptide, ND = not detectable.
704 (c) Representative immunofluorescence staining of CHGA (magenta) in enteroids (whole well)
705 treated with G14, G2D12 and RSP. Boxed portion magnified in lower right corner. Nuclei (4′,6-
706 diamidino-2-phenylindole (DAPI), blue). Scale bars = 1mm and 50μm (boxed portion).
707 (d) Percentage of enteroids with positive CHGA staining in G14, G2D12 and RSP treatments.
708 Table above graph shows the total number of enteroids examined per condition. Average
709 results are from three separate experiments from three different enteroid lines or passages.
710 (e) Left three panels: Representative flow cytometry plots of CHGA+ cells from enteroids grown
711 in G14, G2D12 or RSP. Right panel: Quantification of CHGA+ cells per well. Representative
712 experiment showing n = 3 wells from each condition from a single enteroid line.
713 Bars show mean ± SEM, ***$p < 0.001$, ****$p < 0.0001$. Each experiment repeated with at least
714 three different enteroid lines. Specific conditions were excluded from statistical analysis if the
715 data from 1 or more samples was labeled as not detectable.
716
717
718
719

Figure 3

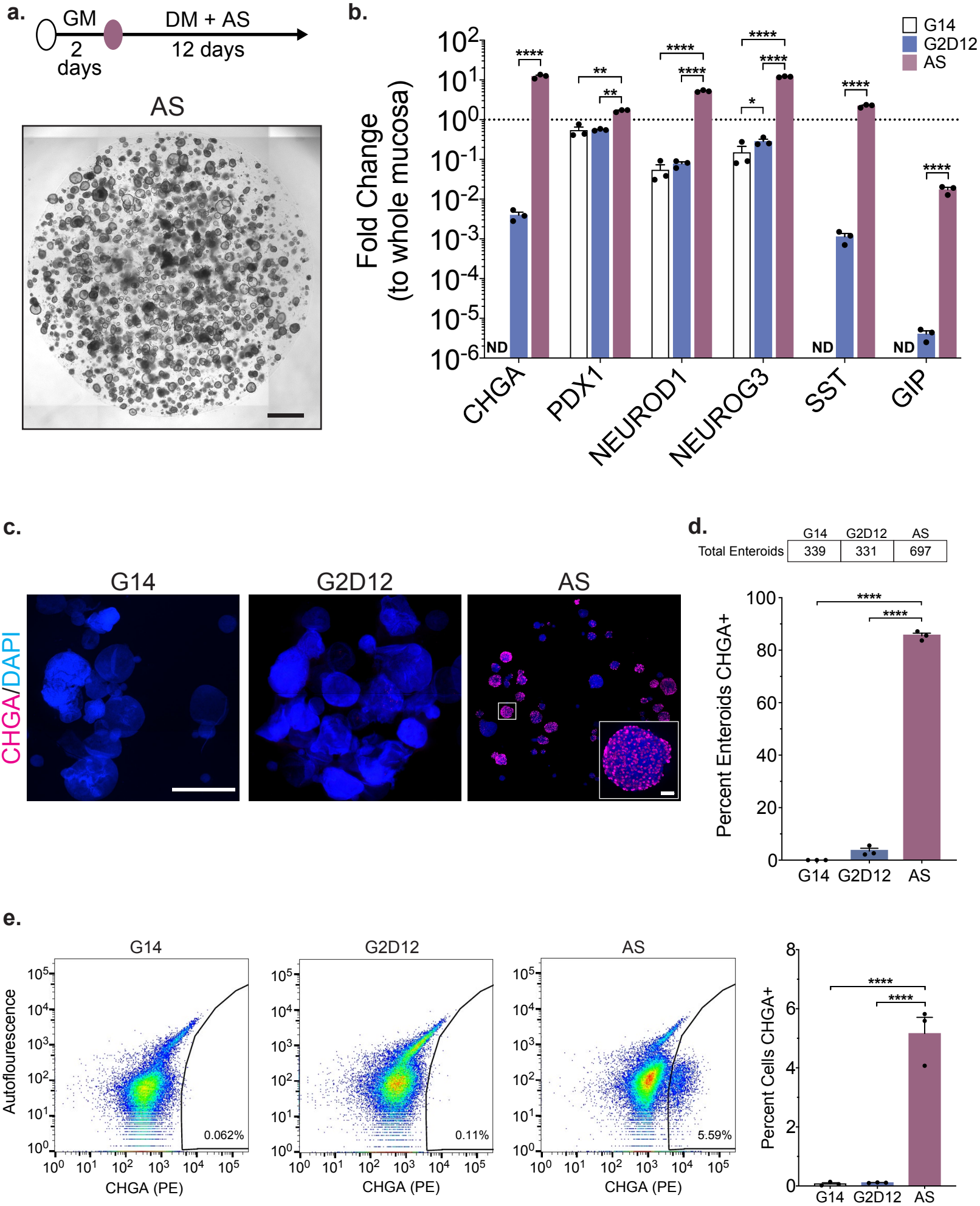

	G14	G2D12	AS
Total Enteroids	339	331	697

720 **Figure 3. Differentiation with Small Molecule AS1842856 Induces CHGA Expression**

721 (a) Representative light microscopy of enteroids (whole well) grown in G2D12 with AS1842856
722 (AS). Culture schematic located above panel. Scale bar = 1mm.

723 (b) qPCR analysis of enteroendocrine markers of enteroids grown in G14, G2D12 or AS
724 compared to whole mucosa and normalized to *18S*. Dotted line denotes expression level in
725 whole mucosa. Representative experiment showing n = 3 wells from each condition from a
726 single enteroid line. CHGA = chromogranin A, PDX1 = pancreatic and duodenal homeobox 1,
727 NEUROD1 = neuronal differentiation 1, NEUROG3 = neurogenin 3, SST = somatostatin, GIP =
728 glucose-dependent insulinotropic peptide, ND = not detectable.

729 (c) Representative immunofluorescence staining of CHGA (magenta) in enteroids (whole well)
730 treated with G14, G2D12 and AS. Boxed portion magnified in lower right corner. DNA (4′,6-
731 diamidino-2-phenylindole (DAPI), blue). Scale bars = 1mm and 50μm (boxed portion).

732 (d) Percentage of enteroids with positive CHGA staining in G14, G2D12 and AS treatments.
733 Table above graph shows the total number of enteroids examined per condition. Average
734 results are from three separate experiments from three different enteroid lines or passages.

735 (e) Left three panels: Representative flow cytometry plots of CHGA+ cells from enteroids grown
736 in G14, G2D12 or AS. Right panel: Quantification of CHGA+ cells per well. Representative
737 experiment showing n = 3 wells from each condition from a single enteroid line.

738 Bars show mean ± SEM, *$p < 0.05$, **$p < 0.01$, ****$p < 0.0001$. Each experiment repeated with
739 at least three different enteroid lines. Specific conditions were excluded from statistical analysis
740 if the data from 1 or more samples was labeled as not detectable.

741

742

743

744

Figure 4

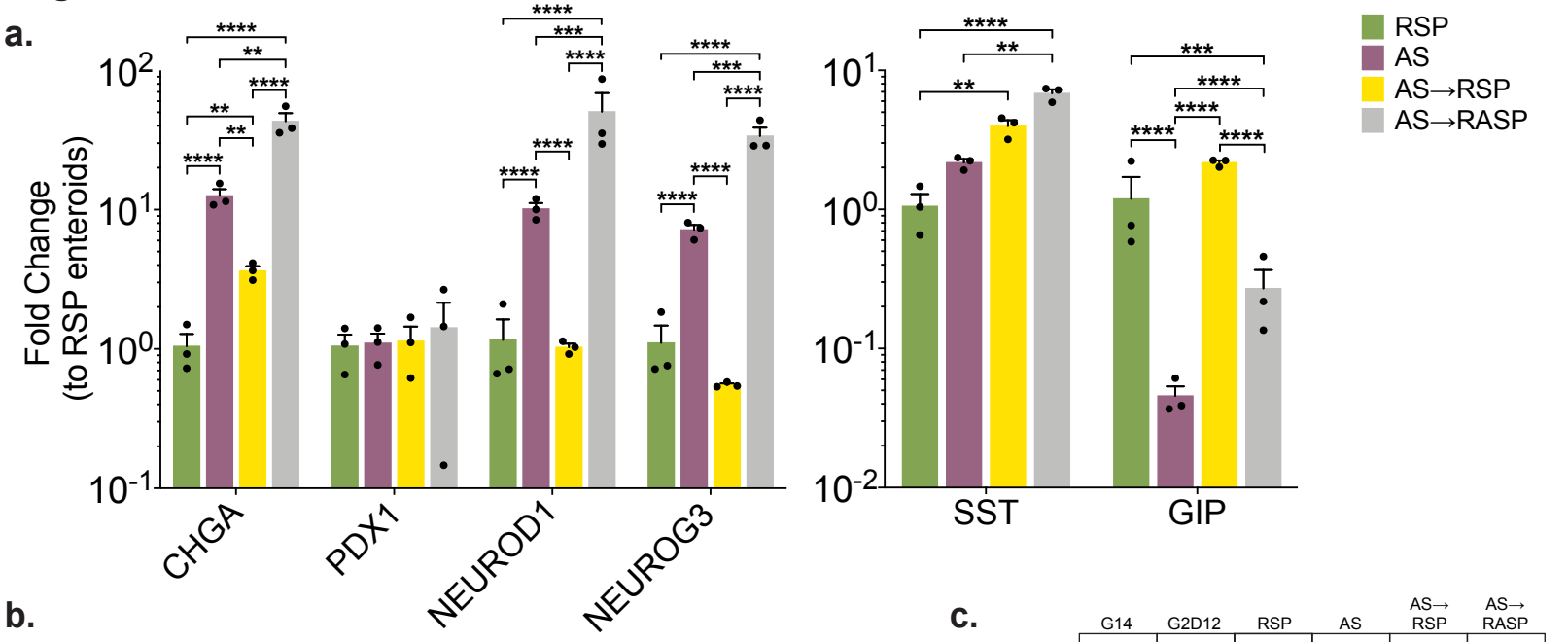

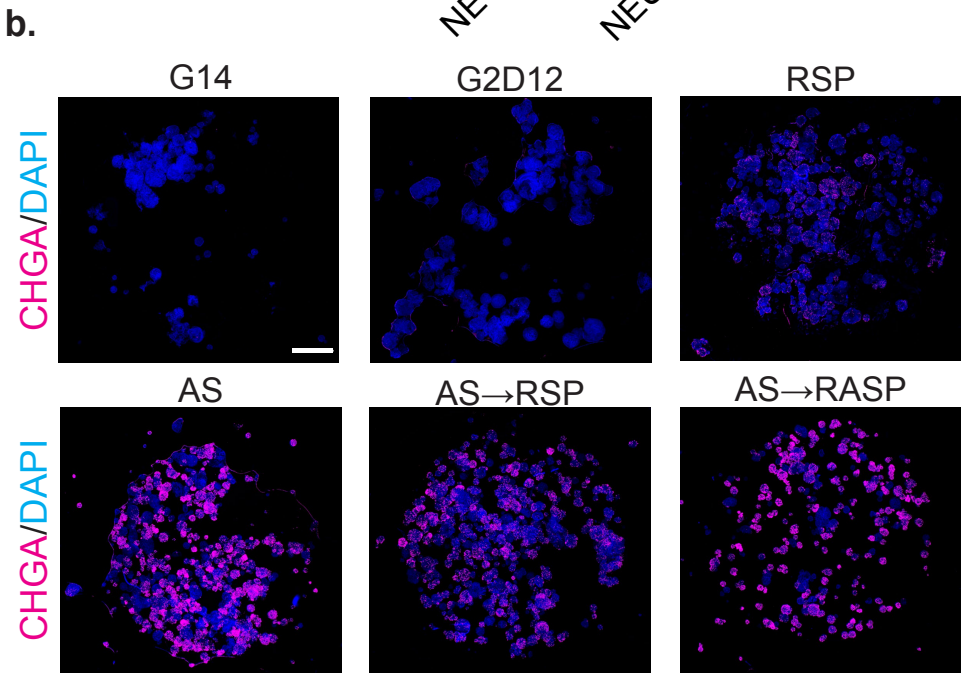

c.

	G14	G2D12	RSP	AS	AS→ RSP	AS→ RASP
Total Enteroids	1070	912	1180	1309	1553	650

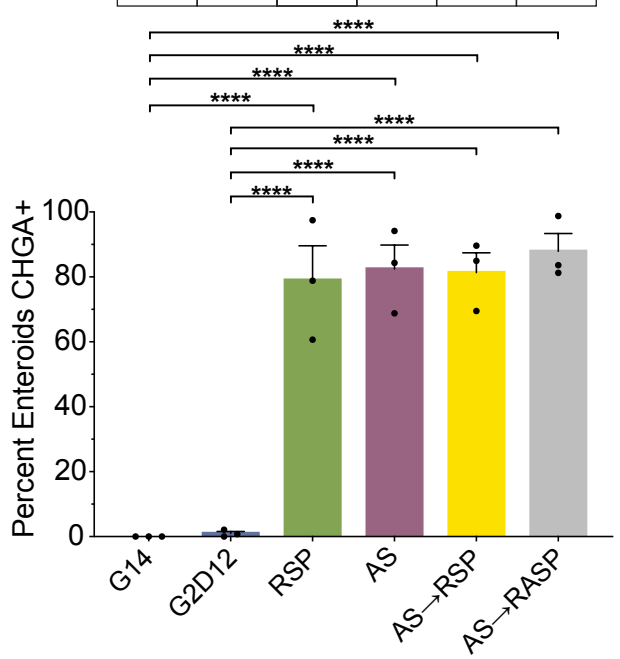

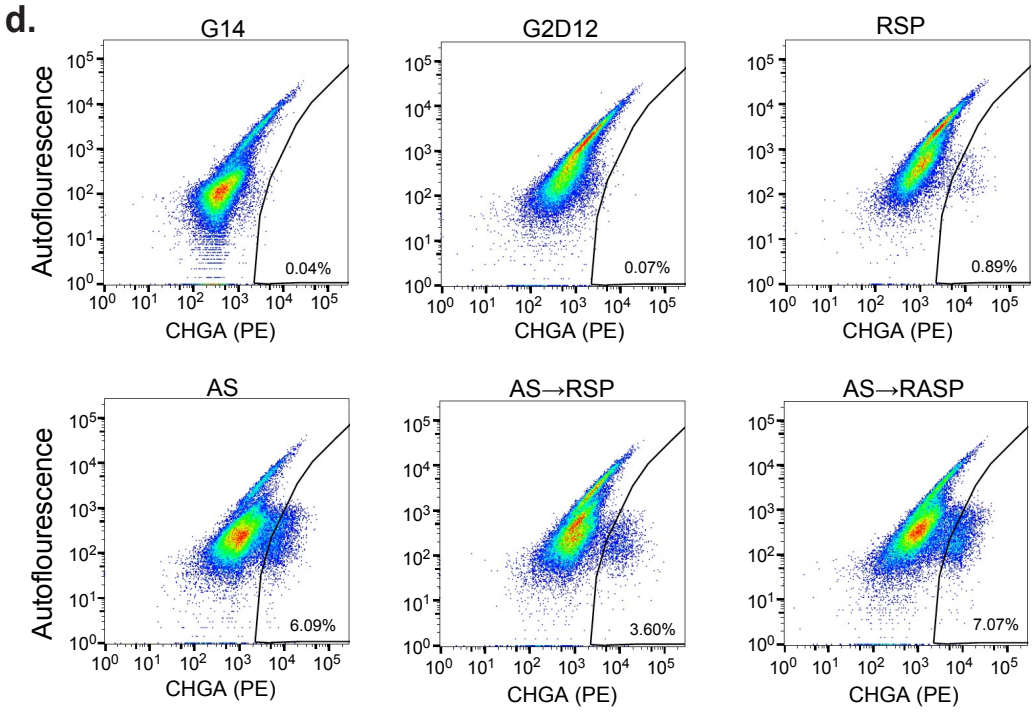

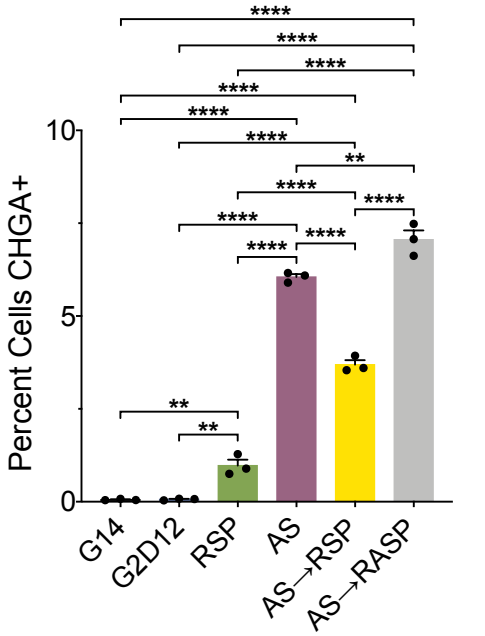

745 **Figure 4. Combinations of AS1842856 and Rimonabant/SP600125 Induce Different Levels**
746 **of Enteroendocrine Marker Expression**
747 (a) qPCR analysis of enteroendocrine markers of enteroids grown in AS, AS for 6 days, followed
748 by RSP only for 6 days (AS→RSP) and AS for 6 days, followed by AS and RSP for 6 days
749 (AS→RASP) compared to enteroids grown in RSP and normalized to *18S*. Representative
750 experiment showing n = 3 wells from each condition from a single enteroid line. CHGA =
751 chromogranin A, PDX1 = pancreatic and duodenal homeobox 1, NEUROD1 = neuronal
752 differentiation 1, NEUROG3 = neurogenin 3, SST = somatostatin, GIP = glucose-dependent
753 insulinotropic peptide.
754 (b) Representative immunofluorescence staining of CHGA (magenta) in enteroids (whole well)
755 treated with G14, G2D12, AS, RSP, AS→RSP, and AS→RASP. DNA (4′,6-diamidino-2-
756 phenylindole (DAPI), blue). Scale bar = 1mm.
757 (c) Percentage of enteroids with positive CHGA staining in G14, G2D12, AS, RSP, AS→RSP,
758 and AS→RASP treatments. Table above graph shows the total number of enteroids examined
759 per condition. Average results are from three separate experiments from three different enteroid
760 lines or passages.
761 (d) Left six panels: Representative flow cytometry plots of CHGA+ cells from enteroids grown in
762 G14, G2D12, AS, RSP, AS to RSP, and AS to RASP. Right panel: Quantification of CHGA+
763 cells per well. Representative experiment showing n = 3 wells from each condition from a single
764 enteroid line.
765 Bars show mean ± SEM, **$p < 0.01$, ***$p < 0.001$, ****$p < 0.0001$. Each experiment repeated
766 with at least three different enteroid lines.
767
768
769

Figure 5

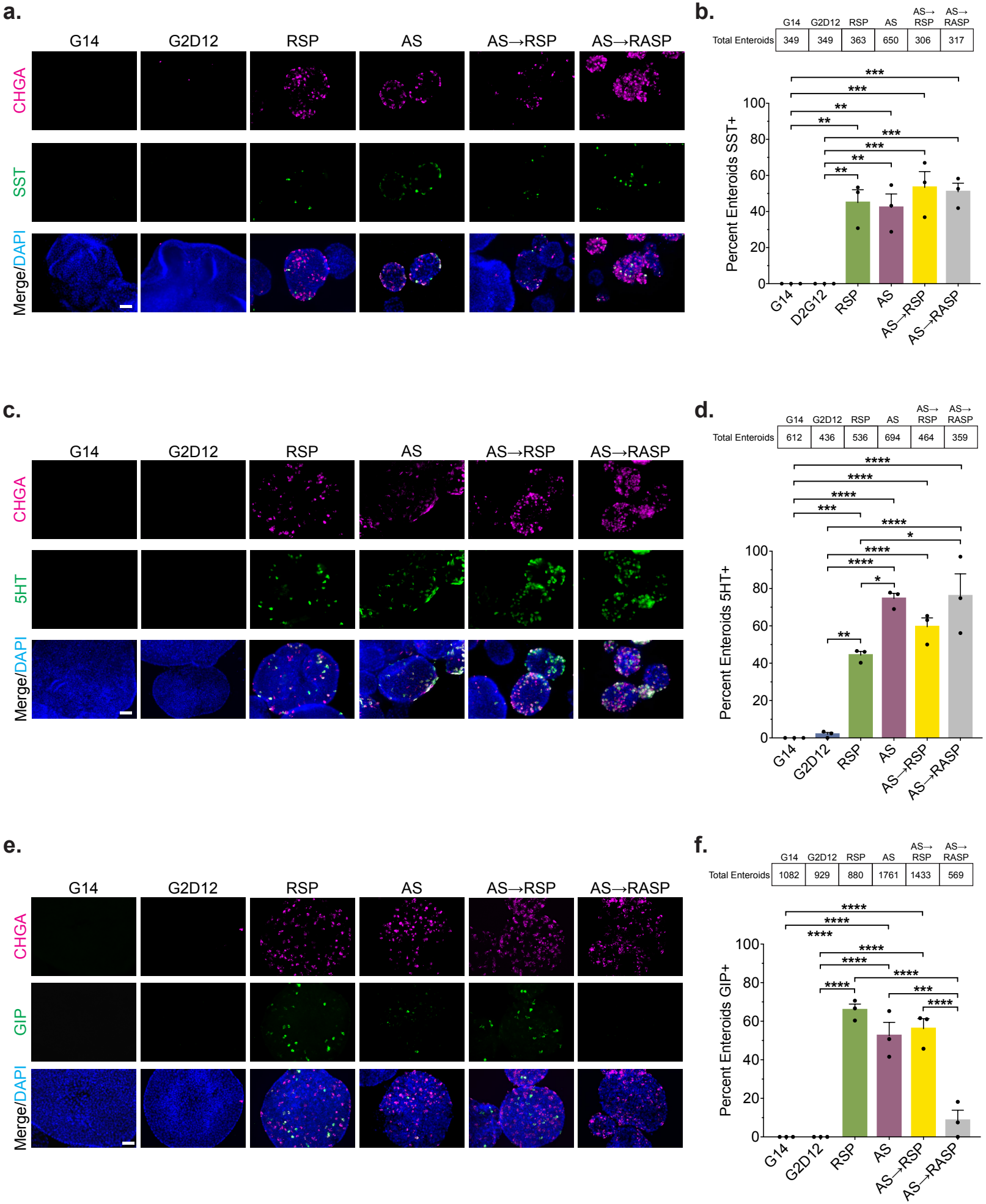
a.
G14
G2D12
RSP
AS
AS→RSP
AS→RASP
CHGA
SST
Merge/DAPI
b.
Total Enteroids
G14 349
G2D12 349
RSP 363
AS 650
AS→RSP 306
AS→RASP 317
Percent Enteroids SST+
c.
5HT
d.
Total Enteroids
G14 612
G2D12 436
RSP 536
AS 694
AS→RSP 464
AS→RASP 359
Percent Enteroids 5HT+
e.
GIP
f.
Total Enteroids
G14 1082
G2D12 929
RSP 880
AS 1761
AS→RSP 1433
AS→RASP 569
Percent Enteroids GIP+

770 **Figure 5. Multiple Differentiation Conditions Induce Hormone Production**

771 (a) Representative immunofluorescence staining of somatostatin (SST, green) and
772 chromogranin A (CHGA, magenta) in enteroids treated with G14, G2D12, AS, RSP, AS→RSP,
773 and AS→RASP. DNA (4′,6-diamidino-2-phenylindole (DAPI), blue). Scale bar = 50μm.

774 (b) Percentage of enteroids with positive SST staining in G14, G2D12, AS, RSP, AS→RSP, and
775 AS→RASP treatments. Table above graph shows the total number of enteroids examined per
776 condition. Average results are from three separate experiments from three different enteroid
777 lines or passages.

778 (c) Representative immunofluorescence staining of serotonin (5HT, green) and chromogranin A
779 (CHGA, magenta) in enteroids treated with G14, G2D12, AS, RSP, AS→RSP and AS→RASP.
780 DNA (4′,6-diamidino-2-phenylindole (DAPI), blue). Scale bar = 50μm.

781 (d) Percentage of enteroids with positive 5HT staining in G14, G2D12, AS, RSP, AS→RSP and
782 AS→RASP treatments. Table above graph shows the total number of enteroids examined per
783 condition. Average results are from three separate experiments from three different enteroid
784 lines or passages.

785 (e) Representative immunofluorescence staining of glucose-dependent insulinotropic peptide
786 (GIP, green) and chromogranin A (CHGA, magenta) in enteroids treated with G14, G2D12, AS,
787 RSP, AS→RSP, and AS→RASP. DNA (4′,6-diamidino-2-phenylindole (DAPI), blue). Scale bar
788 = 50μm.

789 (f) Percentage of enteroids with positive GIP staining in G14, G2D12, AS, RSP, AS→RSP, and
790 AS→RASP treatments. Table above graph shows the total number of enteroids examined per
791 condition. Average results are from three separate experiments from three different enteroid
792 lines or passages.

793 Bars show mean ± SEM, *$p < 0.05$, **$p < 0.01$, ***$p < 0.001$, ****$p < 0.0001$. Each experiment
794 repeated with at least three different enteroid lines.

Figure 6

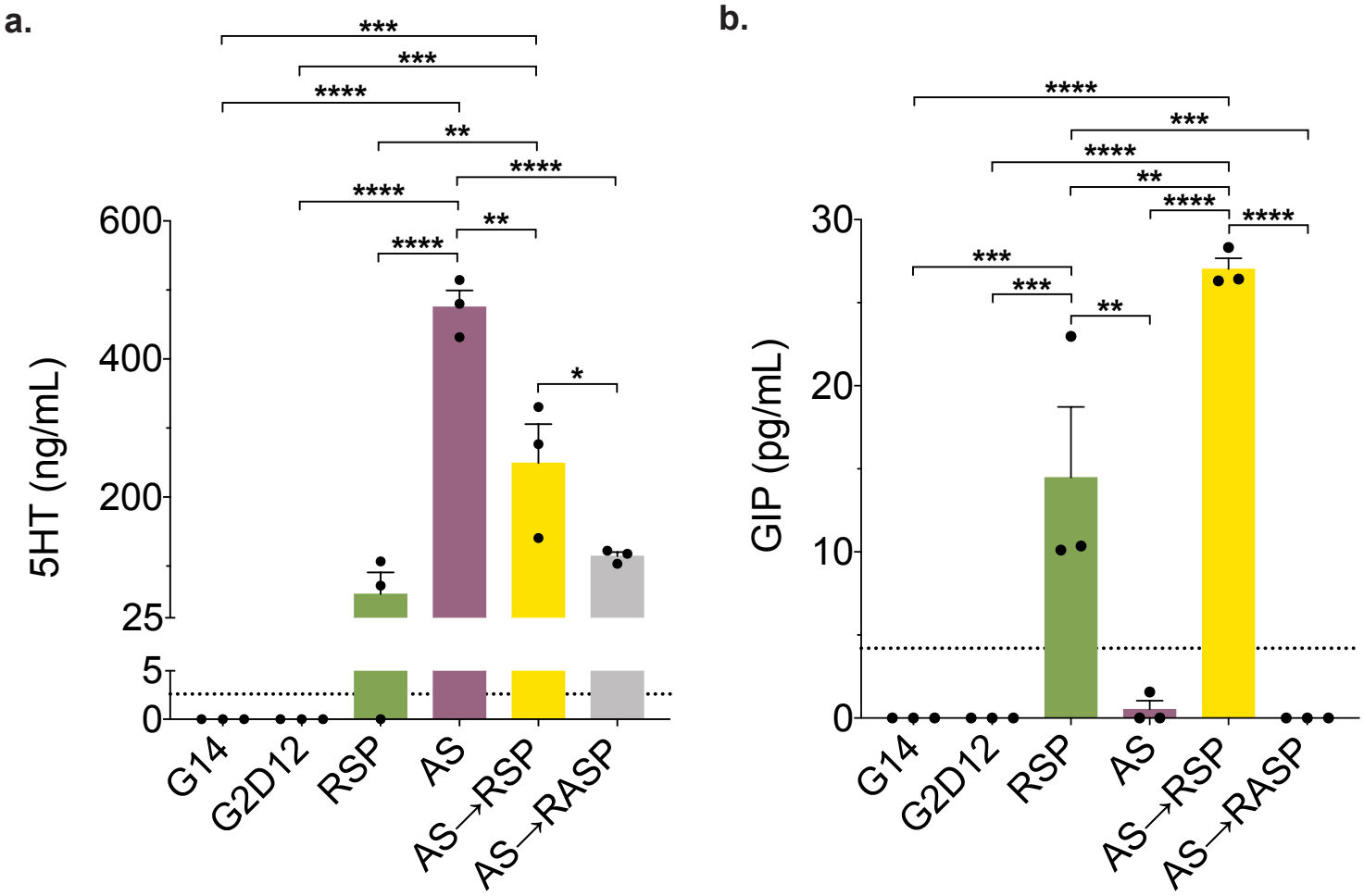
a.
5HT (ng/mL)
600
400
200
25
5
0
***
***
****
**
****
****
**
****
*
G14
G2D12
RSP
AS
AS→RSP
AS→RASP
b.
GIP (pg/mL)
30
20
10
0
****
***
****
**
****
****
***
***
**
G14
G2D12
RSP
AS
AS→RSP
AS→RASP

795 **Figure 6. Differentiation Conditions Induce Hormone Secretion**

796 (a) Serotonin (5HT) ELISA of conditioned media from the last two days of differentiation of
797 enteroids grown in G14, G2D12, AS, RSP, AS→RSP, and AS→RASP. Dotted line at 2.6ng/mL
798 represents the lower limit of detection for the assay. Representative experiment showing n = 3
799 wells from each condition from a single enteroid line.

800 (b) Glucose-dependent insulinotropic peptide (GIP) ELISA of conditioned media from the last
801 two days of differentiation of enteroids grown in G14, G2D12, AS, RSP, AS→RSP, and
802 AS→RASP. Dotted line at 4.2pg/mL represents the lower limit of detection for the assay.
803 Representative experiment showing n = 3 wells from each condition from a single enteroid line.
804 Bars show mean ± SEM, *$p < 0.05$, **$p < 0.01$, ***$p < 0.001$, ****$p < 0.0001$. Each experiment
805 repeated with at least three different enteroid lines.

806

807

808

809

810

811

812

813

814

815

816

817

818

819